



Université Scientifique et Médicale de Grenoble

**INSTITUT DES SCIENCES NUCLEAIRES
DE GRENOBLE**

53, avenue des Morris - BP 257 • 38044 Grenoble Cedex
Tel. 87 71 41

卷之三

¹ See, for example, the discussion of the "right to privacy" in *Privacy and the Constitution* (1985).

[View all posts by \[Author Name\] →](#)

— 1 —

**Laboratoire associé à l'Institut National de Physique Nucléaire
et de Physique des Particules**

FIGURE



FIGURE 1. The value of C_1 as a function of α .

PROOF OF THEOREM 2

Let $\{x_n\}_{n=1}^{\infty}$ be a sequence of points in \mathbb{R}^d such that

Defining $\delta_n = \inf_{x \in \mathbb{R}^d} \|x - x_n\|$, we have

Since $\delta_n > 0$ for all n ,

$$\mathbf{E} \left[\begin{array}{l} \text{Re } C_1(\delta_n) \\ C_1(\delta_n)^2 \\ \text{parameters} \\ \text{G}_1(\delta_n) \end{array} \right] = \begin{cases} \text{Re } C_1(\delta_n) & \text{if } \delta_n < \delta_0 \\ C_1(\delta_n)^2 & \text{if } \delta_n \geq \delta_0 \\ \text{parameters} & \text{if } \delta_n < \delta_0 \\ \text{G}_1(\delta_n) & \text{if } \delta_n \geq \delta_0 \end{cases}$$

the Coulomb barrier. The Coulomb barrier is the potential energy difference between the incident and final states. The Coulomb barrier is given by the formula $V = \frac{Z_1 Z_2 e^2}{r}$, where Z_1 and Z_2 are the atomic numbers of the two nuclei, e is the elementary charge, and r is the distance between the nuclei. The Coulomb barrier is a major factor in determining the cross-section for nuclear reactions. The Coulomb barrier is also important in determining the energy loss of particles passing through matter.

2. Experimental methods

The measurements were performed at the CERN NA3 cyclotron. The 20 Re angular distributions were obtained at 30 MeV on Cu targets at 75 MeV on Cu, Fe, Be, and at 95 MeV on Cu and at 100 MeV on Si. Self-supported natural targets of ^{64}Cu , ^{67}Cu , ^{75}Cu , ^{95}Nb , ^{100}Sn , ^{113}Cd and ^{119}Sn were deposited onto ^{99}Ru cellophane. The 20 Re had a mean charge state of charge state 4^+ for O and 5^+ for the other elements. When the charge state 5^+ was used for 20 Re, the 20 Re ions of charge state 4^+ having the same maximum rapidity were suppressed in the detector by us. Because the energy spectrum of the effects was localized there in 160 Sn group well separated from the 20 Re ones, we could subtract it easily.

11. *U. S. Fish Commission, Annual Report, 1881*, p. 113.

Figure 1. The relationship between the number of species and the area of forest.

¹ Testimony at the hearing before the House Select Committee on Energy Independence and Global Warming, March 10, 2009.

Introducing the new [Kodak EasyShare V1000](#) digital camera.

The Solution Space

Copyright © 2010 by Pearson Education, Inc., or its affiliates. All Rights Reserved.

turns off the CO_2 detector and the pump is turned off.

about 500-1000 nm, and the absorption coefficient is about 10⁻³ cm⁻¹.

¹ See also the discussion of the relationship between the two concepts in the section on "The Concept of Social Capital."

ANSWER $\frac{1}{2} \left(x^2 - 2x + 1 \right) = \frac{1}{2} (x-1)^2$

detritivore (see *detritus*)

(b) $\sin \omega$

For more information about the National Institute of Child Health and Human Development, please call the NICHD Information Resource Center at 301-435-2936 or visit the NICHD Web site at www.nichd.nih.gov.

19. The following table shows the number of hours worked by each employee in a company.

the present paper.

3. Optical and K^{+} - K^{-}

The optical model calculations were performed by means of the SPI code⁶), using a four-parameter potential.

$$V(r) = V_c + (V - V_c)/\epsilon \left[1 - \epsilon^{-1} \frac{r - r_0}{a} e^{\frac{r - r_0}{a}} + \frac{1/\epsilon}{r - r_0} \right],$$

where V_c is the Coulomb potential of a unitary charge distribution of the same radius as the core, by nuclear units.

the energy range of interest. The first step is the one in which the projectile is scattered by the target nucleus. The second step is the one in which the projectile is scattered by the barrier nucleus. The third step is the one in which the projectile is scattered by the target nucleus again. The fourth step is the one in which the projectile is scattered by the barrier nucleus again. The fifth step is the one in which the projectile is scattered by the target nucleus again. The sixth step is the one in which the projectile is scattered by the barrier nucleus again. The seventh step is the one in which the projectile is scattered by the target nucleus again. The eighth step is the one in which the projectile is scattered by the barrier nucleus again. The ninth step is the one in which the projectile is scattered by the target nucleus again. The tenth step is the one in which the projectile is scattered by the barrier nucleus again. The eleventh step is the one in which the projectile is scattered by the target nucleus again. The twelfth step is the one in which the projectile is scattered by the barrier nucleus again. The thirteenth step is the one in which the projectile is scattered by the target nucleus again. The fourteenth step is the one in which the projectile is scattered by the barrier nucleus again. The fifteenth step is the one in which the projectile is scattered by the target nucleus again. The sixteenth step is the one in which the projectile is scattered by the barrier nucleus again. The seventeenth step is the one in which the projectile is scattered by the target nucleus again. The eighteenth step is the one in which the projectile is scattered by the barrier nucleus again. The nineteenth step is the one in which the projectile is scattered by the target nucleus again. The twentieth step is the one in which the projectile is scattered by the barrier nucleus again. The twenty-first step is the one in which the projectile is scattered by the target nucleus again. The twenty-second step is the one in which the projectile is scattered by the barrier nucleus again. The twenty-third step is the one in which the projectile is scattered by the target nucleus again. The twenty-fourth step is the one in which the projectile is scattered by the barrier nucleus again. The twenty-fifth step is the one in which the projectile is scattered by the target nucleus again. The twenty-sixth step is the one in which the projectile is scattered by the barrier nucleus again. The twenty-seventh step is the one in which the projectile is scattered by the target nucleus again. The twenty-eighth step is the one in which the projectile is scattered by the barrier nucleus again. The twenty-ninth step is the one in which the projectile is scattered by the target nucleus again. The thirtieth step is the one in which the projectile is scattered by the barrier nucleus again. The thirty-first step is the one in which the projectile is scattered by the target nucleus again. The thirty-second step is the one in which the projectile is scattered by the barrier nucleus again. The thirty-third step is the one in which the projectile is scattered by the target nucleus again. The thirty-fourth step is the one in which the projectile is scattered by the barrier nucleus again. The thirty-fifth step is the one in which the projectile is scattered by the target nucleus again. The thirty-sixth step is the one in which the projectile is scattered by the barrier nucleus again. The thirty-seventh step is the one in which the projectile is scattered by the target nucleus again. The thirty-eighth step is the one in which the projectile is scattered by the barrier nucleus again. The thirty-ninth step is the one in which the projectile is scattered by the target nucleus again. The forty-thousandth step is the one in which the projectile is scattered by the barrier nucleus again.

For each of the steps in the first two stages of the scattering process, the energy-dependent V_B was calculated by setting only r_0 and α in the potential $V_B(r) = V_0 \exp(-r/r_0) + V_\infty \exp(-r^2/\alpha^2)$ for ^{16}O and $V_B = -V_0 \exp(-r^2/\alpha^2)$ for ^{12}C , respectively. The energy-dependent V_B produced by the scattering parameter r_0 is different from that produced by the other scattering parameters r_0 and α . The energy-dependent V_B produced by the scattering parameter r_0 and α are reported in table 1. The energy-dependent V_B and the corresponding values are approximately the same as those obtained by r_0 and α . It can be noted that for scattering of the smaller ^{12}C nucleus at 100 MeV/u, when the optimum r_0 is greater than $r_{0\mu}$, the optimum α is smaller than $\alpha_{0\mu}$ and vice versa. No such correlation between r_0 and α is clearly observed. The barrier heights V_B deduced from the real potentials are shown in fig. 3. For some projectiles-target combinations, V_B was available at the energies but the values being very close to each other, their mean value was then plotted. The quantity Δr variation of V_B in fig. 3 could be understood simply. In the vicinity of the interaction threshold or near the real nuclear potential P ,

$$V_B + \lambda c P(r) \approx -V_0 \exp(-r_0^{1/3} + \lambda^{1/2}) \frac{r + r_0}{r},$$

the higher V_B is the higher

and

4

as the ratio of the two isotopes in the atmosphere. The ratio of ^{16}O to ^{18}O is approximately 20000 to 1. The oxygen isotope ratio in the precipitation is dependent upon the oxygen isotope ratio in the air at the time of precipitation. The oxygen isotope ratio in the air is dependent upon the oxygen isotope ratio in the water vapor. The oxygen isotope ratio in the water vapor is dependent upon the oxygen isotope ratio in the precipitation. This is a self-reinforcing cycle which results in a steady state condition where the oxygen isotope ratio in the precipitation is approximately 40 times greater than the oxygen isotope ratio in the air.

$\delta_{18}\text{O}$ (per mil)

The ratio of the isotopes of oxygen in the precipitation, ^{16}O and ^{18}O , was well described by the equation $\delta_{18}\text{O} = 10 \log \left(\frac{R_{\text{precip}}}{R_{\text{air}}} \right) - 20$.¹³ It is difficult to read values of $\delta_{18}\text{O}$ from the ratio $R_{\text{precip}}/R_{\text{air}}$ after ^{16}O has presented an appreciable dependence on the temperature, so that good fits could not be obtained with the ratio $R_{\text{precip}}/R_{\text{air}}$ at the depths X and Y when fitted. The parameter $\delta_{18}\text{O}$ derived from $R_{\text{precip}}/R_{\text{air}}$ had a quadratic variation in terms of the parameter $R_{\text{precip}}/R_{\text{air}}^{1/2} + I_y^{1/2}$, in agreement with previous results.¹⁴

The author would like to thank Mr. J. C. G. for his participation in a portion of the present results.

19. *Leucosia* *leucostoma* *leucostoma* *leucostoma* *leucostoma*

TABLE II. The energy levels and wave functions for the ^{16}O , ^{20}Ne , ^{36}Ar , and ^{40}Ca nuclei.

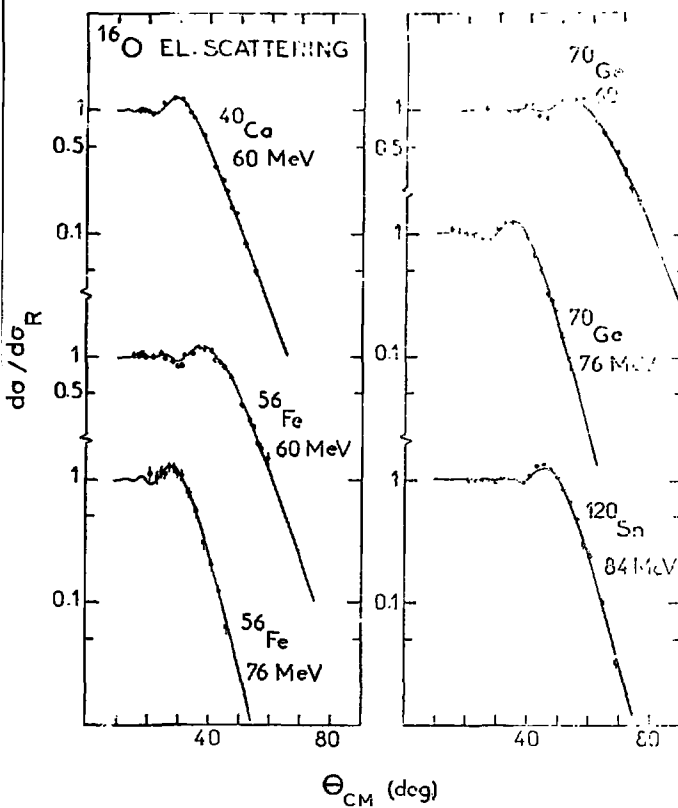
	ℓ_0	ℓ_1	ℓ_2	ℓ_3	ℓ_4	ℓ_5	ℓ_6
^{16}O	0.0	0.0	0.0	0.0	0.0	0.0	0.0
	0.0	0.0	0.0	0.0	0.0	0.0	0.0
^{20}Ne	0.0	1.1	1.1	0.0	0.0	0.0	0.0
	0.0	1.1	1.1	0.0	0.0	0.0	0.0
^{36}Ar	0.0	1.1	1.1	0.0	0.0	0.0	0.0
	0.0	1.1	1.1	0.0	0.0	0.0	0.0
^{40}Ca	0.0	1.1	1.1	0.0	0.0	0.0	0.0
	0.0	1.1	1.1	0.0	0.0	0.0	0.0
L/GSp	1.1	1.1	1.1	0.0	0.0	0.0	0.0

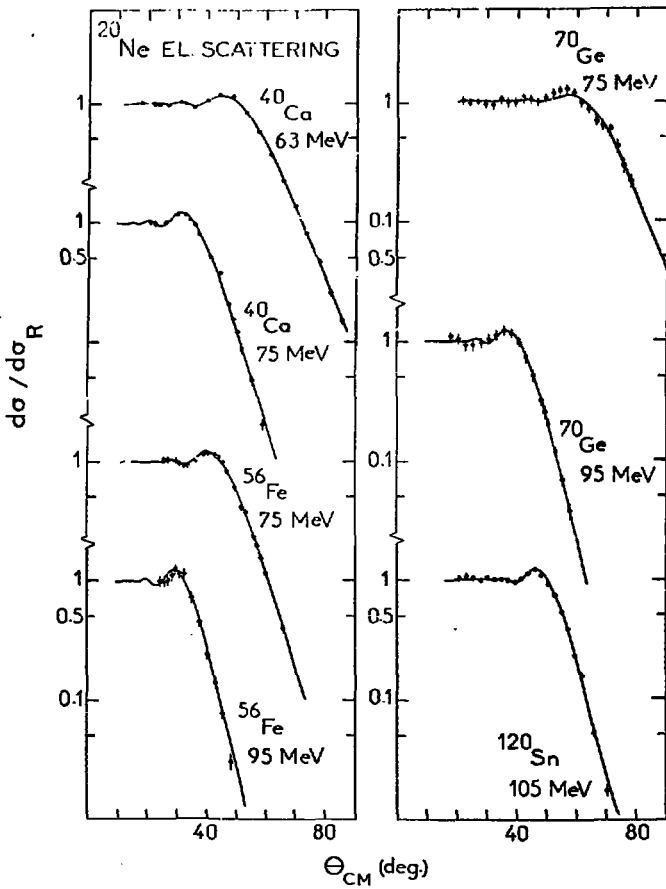
a) with $V = 5 \times 10^{-4}$ and $W = 1 \times 10^{-5}$ for ^{16}O , ^{20}Ne , ^{36}Ar , and ^{40}Ca .

the same time, the ΔE_{ex} value was found to be 1.05 eV. This value is in agreement with the value of 1.06 eV obtained by the same method for the $\text{S}_{\text{2}}\text{O}_8^{2-}$ radical. The spin density distribution of the radical was calculated by the same method as described above. The spin density distribution of the radical is shown in Fig. 1. The spin density distribution of the radical is shown in Fig. 1. The spin density distribution of the radical is shown in Fig. 1.

Figure 2 shows the spin density distribution of the radical. The spin density distribution of the radical is shown in Fig. 2. The spin density distribution of the radical is shown in Fig. 2. The spin density distribution of the radical is shown in Fig. 2.

Figure 3 shows the spin density distribution of the radical. The spin density distribution of the radical is shown in Fig. 3. The spin density distribution of the radical is shown in Fig. 3. The spin density distribution of the radical is shown in Fig. 3.





BARRIER ENERGY (eV)

60
40
20

• ^{16}O
+ ^{20}Ne
○ ^{32}S

20 30 40 50 60 70

$$Z_1 Z_2 / \left(A_1^{1/3} + A_2^{1/3} \right)$$

